FEMS Microbiology Ecology, 92, 2016, fiw111

doi: 10.1093/femsec/fiw111
Advance Access Publication Date: 23 May 2016
Research Article

RESEARCH ARTICLE

Genomic insights into a new acidophilic, copper-resistant *Desulfosporosinus* isolate from the oxidized tailings area of an abandoned gold mine

Andrey V. Mardanov[1], Inna A. Panova[2], Alexey V. Beletsky[1], Marat R. Avakyan[2], Vitaly V. Kadnikov[1], Dmitry V. Antsiferov[2], David Banks[4,†], Yulia A. Frank[2], Nikolay V. Pimenov[3], Nikolai V. Ravin[1] and Olga V. Karnachuk[2,*]

[1]Institute of Bioengineering, Research Center of Biotechnology of the Russian Academy of Sciences, Prosp. 60-let Oktiabria, Building 7-1, 119071 Moscow, Russia, [2]Laboratory of Biochemistry and Molecular Biology, Tomsk State University, Lenina prospect 36, 634050 Tomsk, Russia, [3]Winogradsky Institute of Microbiology, Research Center of Biotechnology of the Russian Academy of Sciences, Pr. 60-letiya Oktyabrya 7/2, 119071 Moscow, Russia and [4]School of Engineering, Systems Power and Energy, Glasgow University, James Watt Building (South), Glasgow G12 8QQ and Holymoor Consultancy Ltd, 360 Ashgate Road, Chesterfield, Derbyshire S40 4BW, UK

*Corresponding author: Laboratory of Biochemistry and Molecular Biology, Tomsk State University, Tomsk 634050, Russia. Tel: +7-382-252-9765; Fax: +7-382-252-9765; E-mail: olga.karnachuk@green.tsu.ru

One sentence summary: A novel acidophilic, copper-tolerant *Desulfosporosinus* sp. I2 has been isolated from oxidized mining waste in Kuzbass; its genome was sequenced and analyzed.

Editor: Tillmann Lueders

†David Banks, http://orcid.org/0000-0002-4575-504X

ABSTRACT

Microbial sulfate reduction in acid mine drainage is still considered to be confined to anoxic conditions, although several reports have shown that sulfate-reducing bacteria occur under microaerophilic or aerobic conditions. We have measured sulfate reduction rates of up to 60 nmol S cm^{-3} day^{-1} in oxidized layers of gold mine tailings in Kuzbass (SW Siberia). A novel, acidophilic, copper-tolerant *Desulfosporosinus* sp. I2 was isolated from the same sample and its genome was sequenced. The genomic analysis and physiological data indicate the involvement of transporters and additional mechanisms to tolerate metals, such as sequestration by polyphosphates. *Desulfosporinus* sp. I2 encodes systems for a metabolically versatile life style. The genome possessed a complete Embden–Meyerhof pathway for glycolysis and gluconeogenesis. Complete oxidation of organic substrates could be enabled by the complete TCA cycle. Genomic analysis found all major components of the electron transfer chain necessary for energy generation via oxidative phosphorylation. Autotrophic CO_2 fixation could be performed through the Wood–Ljungdahl pathway. Multiple oxygen detoxification systems were identified in the genome. Taking into account the metabolic activity and genomic analysis, the traits of the novel isolate broaden our understanding of active sulfate reduction and associated metabolism beyond strictly anaerobic niches.

Keywords: acidophilic sulfate-reducing bacteria; metal resistance; polyphosphates; *Desulfosporosinus*

Received: 8 January 2016; **Accepted:** 20 May 2016

INTRODUCTION

Sulfate-reducing bacteria (SRB) play a vital role in metal detoxification in natural and engineered environments. Hydrogen sulfide, produced by SRB in the course of sulfate respiration, precipitates metals as highly insoluble sulfides. This bioprocess and precipitation can be used in bioreactors to treat metal-contaminated waste streams. Facilitation of microbial sulfate reduction in natural and constructed wetlands is a less costly technique to treat metal-containing effluents as compared to bioreactor processes and chemical and physical abatement. The approach can be applied to treat acid mine drainage (AMD), acidic metal-loaded water produced during coal and metal mining. Major obstacles for microbial treatment are the low pH and high concentration of potentially toxic metals in AMD (Dopson and Johnson 2012; Ňancucheo and Johnson 2014).

SRB have been traditionally regarded as strictly anaerobic organisms. Although our understanding of the aerotolerance of this guild of prokaryotes has changed due to the recent findings in SRB ecology, physiology and biochemistry (reviewed in Cypionka 2000 and Ramel *et al.* 2015), various reports on AMD treatment still consider that sulfate reduction is mostly associated with anaerobic conditions (Meier, Piva and Fortin 2012; Sánchez-Andrea *et al.* 2012, 2014; Ňancucheo and Johnson 2014). The oxidation of dissolved Fe^{2+} to Fe^{3+} is a key biogeochemical process in the metal sulfide-containing wastes. Ferric iron is a more effective chemical oxidant than oxygen. Highly oxidized upper layers of sulfide tailings are rarely regarded as SRB habitats. However, sulfate reduction based on experiments with $^{35}SO_4^{2-}$ has been demonstrated in oxic sediments of AMD-impacted wetlands in the Norilsk area, northern Siberia (Karnachuk *et al.* 2005).

To date, few pure cultures of acidophilic sulfate-reducers have been isolated. Only two acidophilic SRB, *Desulfosporosinus acidiphilus* and *D. acididurans,* have been validly described (Alazard *et al.* 2010; Sánchez-Andrea *et al.* 2015). Deeply branched on the phylogenetic tree, thermophilic *Thermodesulfobium narugense* isolated from a hot spring had a slightly acidic pH optimum between 5.5 and 6.0 for growth (Mori *et al.* 2003). Several *Desulfosporosinus* isolates have been shown to tolerate low pH values (Karnachuk *et al.* 2009, 2015a,b; Abicht *et al.* 2011).

Acidophilic *D. acididurans* was originally isolated from acidic sediments of Rio Tinto and tolerated relatively high concentrations of aluminum and ferrous iron, but was inhibited by 1 mM copper (Sánchez-Andrea *et al.* 2015). The tolerance to metal ions has not been reported for *D. acidiphilus*, isolated from AMD-impacted sediments in France (Alazard *et al.* 2010), or for *T. narugense* (Mori *et al.* 2003). Acidophilic *Desulfosporosinus* sp. OT, resistant up to 236 mM copper, was isolated from a gold mine site in Kuzbass, southwestern Siberia and its draft genome has been published (Abicht *et al.* 2011). The draft genome of the only deltaproteobacterial acid-tolerant *Desulfovibrio* sp. TomC has also been published (Karnachuk *et al.* 2015c). Our recent findings showed that strain TomC is sensitive to Cu^{2+} at concentrations higher than 1.5 mM (Karnachuk *et al.*, unpublished data). A neutrophilic *Desulfovibrio* sp. A2 could tolerate up to 12.6 mM Cu^{2+} (Mancini *et al.* 2011). At present, four complete and three draft *Desulfosporosinus* genomes have been announced (Abicht *et al.* 2011; Pester *et al.* 2012; Abu Laban *et al.* 2015; Petzsch *et al.* 2015b), but the metabolism and other traits have not been analyzed.

The purpose of this study was to measure sulfate reduction in oxic layers of a tailings site of an abandoned gold mine and to characterize sulfate reducers at this site. A copper-tolerant, acidophilic SRB was isolated from the same sample that was used for the *in situ* sulfate reduction rate measurements and its genome was sequenced. Genome data are analyzed to provide insights into the metabolism of the isolate and outline putative mechanisms of its resistance to heavy metals, low pH and oxidative stress.

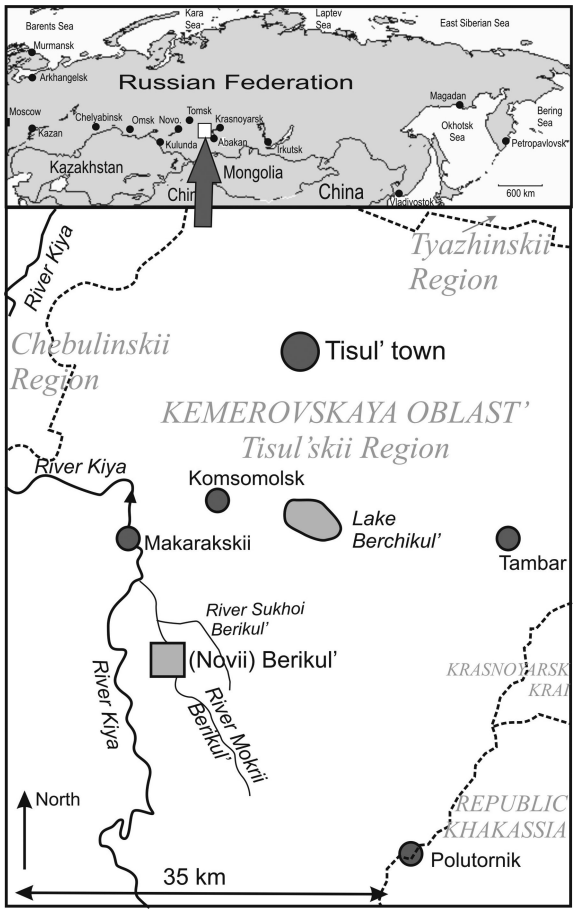

Figure 1. Location map. The white rectangle in the upper map shows the location of the study area within the Russian Federation. The mine tailings are located at the Novii Berikul' processing works.

MATERIALS AND METHODS

Site description

The Kuznetsk mining area (commonly known as the 'Kuzbass') is located in southwestern Siberia, Russia, and is one of the world's main sources of coal. Iron and non-ferrous metal sulfides are also mined in the region. Gold mining in the Mariinskaya Taiga ('Martaiga') area of the Kuzbass dates back to the early part of the 19th century. Geologically, the region comprises a bedrock terrain of the Kuznetsk Alatau mountain belt (Fig. 1; Banks *et al.* 2008). The mining area is associated with quartz-sulfide ore deposits with a high content of arsenopyrite.

Underground mines at the Berikul site were reportedly worked down to 500 m deep in a polymetallic sulfide-quartz-pyrite/arsenopyrite-gold deposit, but were mined only for gold. Ore material from the mines was transported to the processing works on the west bank of the Mokrii Berikul River. The processing works included milling, flotation and cyanidation. The waste materials (tailings from all the stages) were deposited on the river bank and separated by a dam. The tailings have been present since 1952 and comprise 40%–45% fine-grained

Table 1. Redox potential and sulfate reduction rates in Xa201 and Xa202 sediment samples.

Sampling site	Depth, cm	Eh, mV	SRR (±SD), nmol S cm^{-3} day^{-1}
Xa201	0–0.4	265	17.6 ± 2.4
Xa201	0.5–3	110	8.72 ± 1.7
Xa202	0–0.5	456	1.69 ± 0.4
Xa202	1–3	380	60.0 ± 8.5

sulfide (dominated by pyrite, with minor arsenopyrite and smaller amounts of pyrrhotite, sphalerite, chalcopyrite, galena, quartz, albite, chlorite, muscovite and dolomite) as reported by Sidenko *et al.* (2005). The mine was closed in 1994, and parts of the mine waste materials and tailings were removed from the site in the late 1990s–early 2000s and covered by a layer of coarse-grained mine waste rock. The remaining materials in the tailings still undergo oxidation, as evidenced by many orange–yellow pools of accumulated leachate. Highly acidic, metal-laden leachate from the tailings has been a matter of environmental concern over the years (Bortnikova *et al.* 2001; Gieré, Sidenko and Lazareva 2003; Sidenko *et al.* 2005).

Sampling, field measurements, water and sediment analyses

The samples were collected on 26 August 2007 from two different pools in the tailings area (Table 1). The sampling site Xa201 was at the foot of a mine waste pile, while Xa202 was located on the flood plain of the Mokrii Berikul River. The upper layer of the sediment was grab sampled, while deeper layers were sampled from sediment cores retrieved with a Plexiglas tube. Redox potentials were measured on-site by inserting the electrodes (HANNA HI8314F) (Hanna Instruments, Germany) into the water-saturated sediments.

Water for chemical analysis was filtered into 50 ml polyethylene flasks, using a Millipore filter (0.45 μm pore size) and a hand-held polypropylene syringe. No acidification was carried out in the field. For the pH and other field measurements, electrodes were submerged to the maximum extent below to water surface (typically 5–10 cm). Two samples of filtered water from each site were transported to the analytical laboratory of the Hydrochemical Engineering Research and Outreach Group at the University of Newcastle for chemical analysis. Prior to analysis, samples were stored at 4°C except for brief periods of transportation. Anion concentrations were determined by ion chromatography (Dionex DX320 for Gradient Anion Analysis) (Thermo Fisher Scientific/Dionex, Sunnyvale, California) from split samples from both sites. Other split samples were acidified with concentrated ultrapure HNO_3 in order to redissolve any precipitated or sorbed metals and analyzed using inductively coupled plasma-atomic emission spectrometry (Varian Vista, Varian Inc., Palo Alto, California, MPX with a simultaneous charged coupled device).

The mineralogical composition of the upper layers of Xa201 and Xa202 sediments was characterized by X-ray diffraction (XRD) using a Shimadzu XRD-6000 (Shimadzu Corporation, Kyoto, Japan) diffractometer as previously described (Ikkert *et al.* 2013). For scanning electron microscopy (SEM), air-dried sediments were examined under a Philips SEM 515 (Philips, Electronic Instruments, Eindhoven, The Netherlands) scanning electron microscope. Energy dispersive spectrometry (EDS; EDAX Inc., Mahwan, NJ) was performed at a voltage of 30 kV and a working distance of 12 mm. For transmission electron microscopy (TEM) ultrathin sections of the cells were prepared as previously described (Ikkert *et al.* 2013). Sections were viewed under a JEM-100 CXII electron microscope (JEOL, Tokyo, Japan) at 80 kV.

Sulfate reduction rate measurements

For the measurement of sulfate reduction rates, aliquots of sediments were withdrawn using sterile plastic syringes, with the tips clipped off, from the middle of the cores or grab samples. Samples in syringes were tightly end-sealed with butyl rubber stoppers. Aliquots (100 μl) of $Na_2{}^{35}SO_4$ (15 μCi, Isotop, Obninsk, Russia) in degassed sterile 0.002% resazurin solution were injected into syringes vertically along the center of the core through the butyl rubber stoppers as described earlier (Karnachuk *et al.* 2006). All sulfate reduction rate measurements were carried out in triplicates. The samples were incubated in the dark at *in situ* temperature for 24 h. One milliliter of 2 M KOH was used to terminate the incubation and to fix sulfide. The total amount of reduced ^{35}S was measured as the sum of the acid volatile fraction and chromium-reducible sulfur as described previously (Karnachuk *et al.* 2005, 2006).

SRB enrichment and pure culture isolation

Enrichment cultures were initiated with inoculations from the Xa201 surface layer sediments within 3–4 days after the sampling. Samples were stored at 4°C prior to inoculation. Widdel and Bak medium (Widdel and Bak 1992) modified for copper-tolerant SRB isolation (Karnachuk *et al.* 2008) was used to set up initial enrichments with glycerol as an electron donor. The pH was adjusted to 2.0 with 1 M H_2SO_4 solution. No special buffer solutions were used to maintain an acidic pH. The enrichment cultures were incubated at 28°C. The final pH values of the enrichments were between 4 and 5. A pure culture was isolated by repeated serial dilutions with glycerol as an electron donor following heat treatment at 95°C for 20 min.

For substrate utilization tests the isolate was grown in sealed, headspace-free test tubes. Electron donors were tested at final concentrations of 25 mM ethanol, 18 mM lactate, 13.5 mM butanol, 8 mM nicotinic acid, 11 mM glycerol, 5 mM citrate, 4.5 mM succinate, 3 mM sucrose, 1 mM palmitate, 9 mM each of acetate and fumarate, 7.5 mM each of formate and malate, 7 mM each of pyruvate and butyrate, 5 mM each of fructose and glucose (all Sigma-Aldrich, St. Louis, MO, USA). Peptone (1%) was also used as an electron donor. Carbohydrate stock solutions were filter-sterilized. The cultures were subcultured at least five times to confirm that they utilized the test compounds.

DNA isolation, genome sequencing, assembly and annotation

For DNA isolation the isolate was grown at 28°C in freshwater Widdel and Bak medium modified with glycerol and sulfate for copper-resistant SRB (Karnachuk *et al.* 2008). Cells were collected by centrifugation, resuspended in Tris-EDTA (TE) buffer (10 mM Tris; 1 mM EDTA (Merck, Darmstadt, Germany), pH 8.0) and lysed with sodium dodecyl sulfate (SDS) (Sigma-Aldrich, St. Louis, MO, USA) and Proteinase K (Qiagen, Hilden, Germany). DNA was purified by Cetyl trimethylammonium bromide (CTAB) and phenol:chloroform:isoamyl alcohol extractions and precipitated with ethanol.

Genomic DNA was sequenced with a Roche Genome Sequencer (GS FLX) (454 Sciences, Branford, CT, USA) using the XL+ protocol. About 186 MB of a shotgun library sequences were produced with an average read length of 704 bp. The GS FLX reads were assembled using Newbler assembler version 2.9 (454 Life Sciences, Branford, CT). The draft genome of *Desulfosporosinus* sp. I2 consists of 318 contigs longer than 500 bp, with a total length of 5311 733 bp.

Coding genes were annotated using RAST server (Brettin *et al.* 2015) and manually curated. The tRNAScanSE tool (Lowe and Eddy 1997) was used to find tRNA genes, whereas ribosomal RNA genes were found by RNAMMER (Lagesen *et al.* 2007). The annotated genome sequence of *Desulfosporosinus* sp. I2 has been deposited in the GenBank database under accession no. NZ_JYNH00000000.

RESULTS

Water and sediment analyses and sulfate reduction rates

Both tailings leachates were highly acidic, pH 2.5 at the Xa201 site and pH 3.6 at the Xa202 site (Table S1, Supporting Information). Sulfate was the major anion with the concentration of 5290 mg SO_4 l^{-1} in Xa201 and 7790 mg SO_4 l^{-1} in Xa202 (Table S2, Supporting Information). The water samples were also rich in dissolved iron, with concentrations of up to 2290 mg Fe l^{-1} in Xa202. The samples also contained high concentrations of other dissolved metals; e.g. 242 mg l^{-1} Al (Xa202), 162 mg l^{-1} Zn (Xa201), 12.5 mg l^{-1} Cu (Xa201), 5 mg l^{-1} Ni (Xa202) and 2.8 mg l^{-1} Cd (Xa201). The concentration of arsenic was 178 mg l^{-1} in the Xa201 leachate and 6.5 mg l^{-1} in Xa202.

Muscovite, albite and quartz were the main Si minerals derived from the gangue material in Xa201 and Xa202 sediments (Fig. S1, Supporting Information). Crystalline Fe-sulfides or other sulfide minerals were not detected in either sample. Arsenic sulfides, including orpiment (As_2S) and realgar (AsS), were present as minor phases in Xa202 sediment. Various forms of secondary sulfates, including a jarosite-type phase and melanterite, were also detected in the sediment samples.

SEM-EDS analysis showed that two major types of fine-sized grains occurred in Xa201 and Xa202 sediments. One type of grain was smooth-surfaced (Fig. S2A, Supporting Information) and exhibited two major EDS peaks of Si and O, suggesting that this type represents quartz. The other type of the sediment grain was intensively weathered and covered by filaments and spheres (Fig. S2B–F, Supporting Information). The EDS spectra showed enrichment in C, which implies that the filaments may be mineralized microbial cells.

The intense orange–yellow color and positive Eh values measured in the top and subsurface layers (Table 1) were a clear indication of an oxidizing environment in the top layers of the pool sediments. The highest sulfate reduction rate, 60.0 nmol S cm^{-3} day^{-1}, was detected in the subsurface layer of Xa202, whereas the lowest value 1.69 nmol S cm^{-3} day^{-1} was measured in the top layer of this pool (Table 1). The sulfate reduction rate observed in Xa201 sediment was the same order of magnitude and showed little variation with depth, reaching 17.6 nmol S cm^{-3} day^{-1} in the upper layer and 8.72 nmol S cm^{-3} day^{-1} in the lower 0.5–3 cm horizon.

SRB pure culture isolation and characterization

The initial SRB enrichment was grown in the presence of 200 mg Cu l^{-1}. The strain, designated I2, was obtained by repeated serial dilutions with glycerol as an electron donor following heat treatment at 95°C for 20 min.

Strain I2 is slightly curved motile rods, 3–6 μm long and 0.5–1.0 μm wide (Fig. 2). Cells stained Gram-negative, although the absence of a discreet outer membrane indicates a Gram-positive wall structure. Paraterminal oval spores slightly swelling the cell are often present. Electron micrographs of ultrathin sections revealed a thin peptidoglycan layer and a lighter outer, presumably an S-layer (Fig. 2a). The cytoplasmic membrane has deep invaginations (Fig. 2b). The extensive inner membrane excrescence occurred at the cell poles and appeared as rings on the cross sections (Fig. 2a). Large (up to 0.5 μm in diameter) electron-transparent vacuole-like globules were present in cells grown in the presence of 25 mg Cu l^{-1} (Fig. 2c and d). The globules may be surrounded with a membrane (Fig. 2d). When cells were grown in the presence of 25 and 150 mg Cu l^{-1}, the globules engulfed a network of electron-dense fibrils (Fig. 2e and f). The numerous observations of the fibrils in cells growing at elevated copper concentrations suggest that it was not an artifact of staining (Fig. S3, Supporting Information).The fine electron-dense fibrils also surrounded the cell wall (Fig. 2f–h). The presence of polyphosphate (polyP) in the cells was revealed both by methylene blue and Neisser staining (data not shown).

Strain I2 is psychrotolerant, growing at the temperature range 4°C–32°C with the optimum at 22°C–28°C. The strain did not grow under microaerophilic conditions, when cells were cultivated in stoppered vials containing 6 ml liquid medium and 6 ml ambient air in the headspace. Strain I2 could use lactate, pyruvate, malate, citrate, succinate, fumarate, butyrate, ethanol, glycerol, butanol, formate, palmitate, and peptone as electron donors for sulfate reduction. The strain did not grow with fructose, glucose, sucrose, acetate or nicotinic acid in sulfate medium. Pyruvate and lactate supported fermentative growth without sulfate. Fumarate and nitrate in addition to sulfate could be used as electron acceptor. The strain did not grow with nitrite as an electron acceptor.

Strain I2 could grow at initial Cu^{2+} concentration of up to 142 mM and the pH range from 1.7 to 7.0. The pH of the medium increased during the growth and the copper concentration decreased due to CuS precipitation. The medium with initial pH 7.3 and higher did not support growth. The maximum cell numbers and the shortest lag phases were observed at initial pH 2.6. The tolerance to other divalent metals was much lower. The initial concentration of metals allowing growth did not exceed 2.7 mM for Cd^{2+}, 8.5 mM for Ni^{2+} and 8.5 mM for Co^{2+}. Arsenate inhibited growth at concentrations higher than 0.2 mM (15 mg l^{-1}).

Phylogenetic analysis of the 16S rRNA gene of strain I2 places it within the phylum Firmicutes, class Peptococcaceae, genus *Desulfosporosinus* (Fig. 3). *Desulfosporosinus burensis* was the closest relative with the sequence identity of 98%.

Genome properties

Pyrosequencing and assembly of the draft genome of *Desulfosporosinus* I2 yielded 318 contigs longer than 500 bp with N50 contig size of 30 483 bp. The size of the genome, estimated as a total length of all contigs, is about 5.3 Mbp, and the GC content of the genome is 42.04%. Five copies of the 16S-23S-5S rRNA operon and 43 tRNA genes coding for all 20 amino acids were identified. Annotation of the genome sequence revealed 5512 potential protein-coding genes of which 3987 (72%) can be functionally assigned. Analysis of the conserved single-copy marker genes using CheckM (Parks *et al.* 2015) estimated the

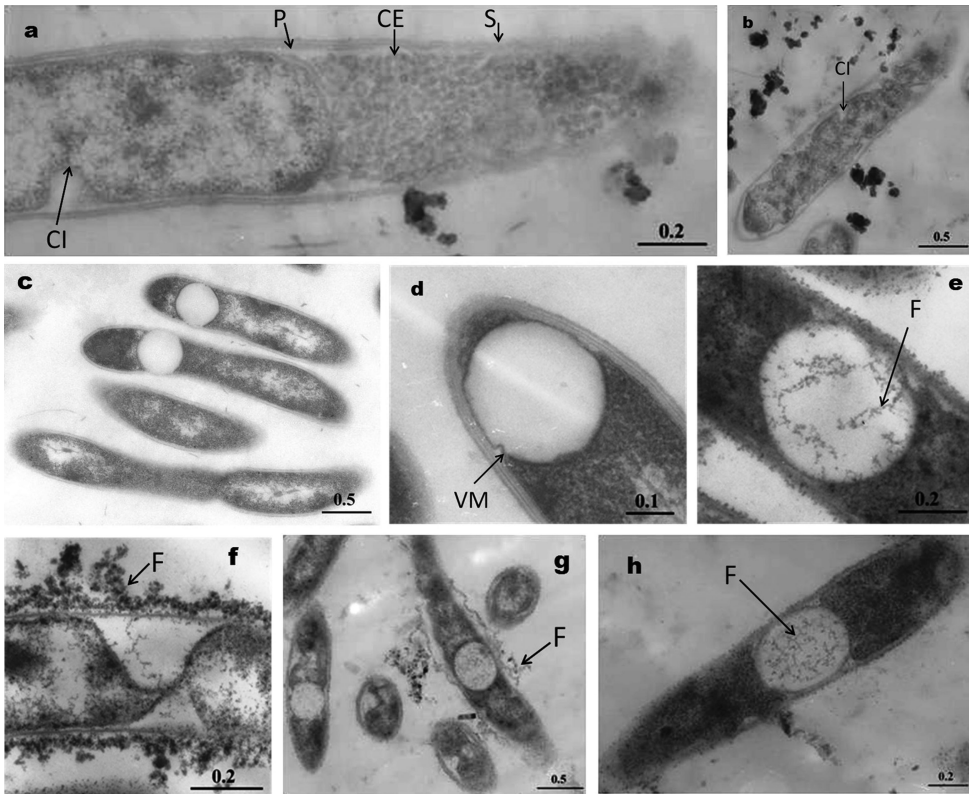

Figure 2. TEM micrographs of ultrathin sections of strain I2 grown without copper addition (**a**, **b**); vacuole-like inclusions in cells growing with initial copper concentration of 25 mg/l (**c**, **d**); electron-dense fibrils in the inclusions (**e**) and associated with the cell wall (**f**) in cells growing with initial copper concentration of 25 mg/l; extensive fibrils in the inclusions in the cells growing with initial copper concentration of 150 mg/l (**g**, **h**). C, cytoplasmic membrane; CE, cytoplasmic membrane extensions; CI, cytoplasmic membrane invaginations; P, peptidoglycan; S, presumed S-layer; F, fibrils; VM, vacuole membrane. The scale bars are given in micrometer.

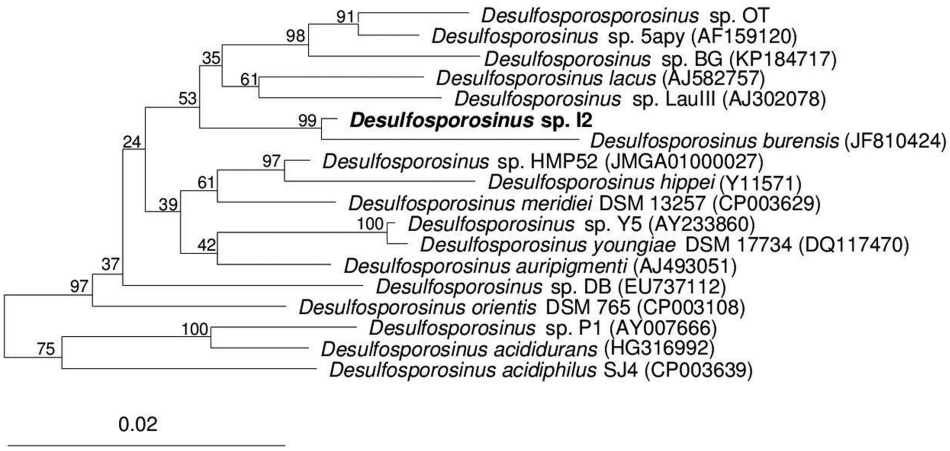

Figure 3. Neighbor-joining 16S rRNA tree showing the phylogenetic position of *Desulfosporosinus* I2, validly described members of *Desulfosporosinus*, and several unidentified strains. *Desulfotomaculum acetoxidans* DSM771 (not shown) was used as an outgroup. Numbers at branching points indicate bootstrap values determined from 1000 iterations. The scale bar represents an estimated 2% sequence divergence.

completeness of this draft genome as 98%. The size of the *Desulfosporosinus* I2 genome is comparable to that of complete genomes of other *Desulfosporosinus* spp. (4.9–5.9 Mbp; Pester *et al.* 2012).

Resistance to heavy metals and arsenate

All three mechanisms of resistance to the metal stress (Nies 2003), P-type ATPases, RND (resistance-nodulation-cell division) transporters and cation diffusion facilitators (CDF) were revealed in the strain I2 genome (Table 2). Two operons comprise copper/silver ATPases CopA (UF75_1662, UF75_4258), transcriptional regulators CsoR (UF75_1661, UF75_4257) and one of the operons also contained a copper chaperon CopZ (UF75_1663). The genome contains two RND-family efflux transporter genes (UF75_0596, UF75_1490), linked to MFP (membrane fusion protein) genes (UF75_0597, UF75_1491). In addition to the family of P-type ATPases transporting Cu and Ag ions, strain I2 possesses the second family of heavy metal P-type ATPases,

Table 2. Description of the genes related to metal tolerance.

				Closest relative			
Gene ID	Accession no.	Size/aa	Predicted function	Organism	Identity	Size/aa	Accession no.
Heavy metal transporting P-type ATPases							
UF75_0864	WP_045573304	735	Heavy metal translocating P-type ATPase	*Desulfitobacterium dichloroeliminans*	69%	808	WP_015261865
UF75_1661	KJR47987	115	Repressor CsoR of the copZA operon	*Desulfosporosinus* sp. BICA1-9	92%	114	WP_034143585
UF75_1662	WP_045574022	914	Copper-translocating P-type ATPase CopA	*Desulfosporosinus* sp. BICA1-9	85%	920	WP_034143564
UF75_1663	WP_045574023	65	Copper chaperon CopZ	*Desulfosporosinus* sp. BICA1-9	94%	66	WP_034143565
UF75_1937	WP_045574273	624	Heavy metal translocating P-type ATPase	*Desulfosporosinus* sp. OT	89%	624	WP_009624106
UF75_3100	KJR46488	790	Heavy metal translocating P-type ATPase	*Desulfosporosinus* sp. BICA1-9	93%	779	WP_034143029
UF75_3101	KJR46489	94	DNA-binding transcriptional regulator, ArsR family	*Desulfosporosinus* sp. BICA1-9	97%	121	WP_034143024
UF75_3331	WP_045575489	894	Magnesium-transporting P-type ATPase	*Desulfosporosinus* sp. BICA1-9	91%	894	WP_034145514
UF75_3976	WP_045576049	86	Copper chaperon CopZ	*Desulfosporosinus* sp. BICA1-9	91%	87	WP_034144231
UF75_4257	WP_045576280	111	Repressor CsoR of the copZA operon	*Desulfosporosinus* sp. HMP52	82%	112	WP_034601390
UF75_4258	KJR45355	859	Copper-translocating P-type ATPase CopA	*Desulfosporosinus* sp. HMP52	93%	841	WP_034599599
UF75_4472	WP_045576455	782	Heavy metal translocating P-type ATPase	*Desulfosporosinus* sp. BICA1-9	95%	779	WP_034143029
UF75_4473	WP_045576456	121	DNA-binding transcriptional regulator, ArsR family	*Desulfosporosinus* sp. BICA1-9	98%	121	WP_034143024
UF75_5045	WP_045576951	111	Repressor CsoR of the copZA operon	*Desulfosporosinus* sp. HMP52	81%	112	WP_034601390
RND-family efflux pumps							
UF75_0168	WP_045572694	373	RND-family efflux transporter, MFP subunit	*Desulfosporosinus youngiae*	70%	400	WP_007786850
UF75_0596	WP_045573056	1021	RND-family efflux transporter protein, subunit AcrB	*Desulfosporosinus* sp. BICA1-9	87%	1027	WP_034145430
UF75_0597	KJR49082	361	RND-family efflux transporter, MFP subunit	*Desulfosporosinus* sp. BICA1-9	82%	361	WP_034141772
UF75_1490	WP_045573879	1043	RND-family efflux transporter protein, subunit AcrB	*Desulfosporosinus* sp. OT	84%	1043	WP_009618874
UF75_1491	KJR48138	404	RND-family efflux transporter, MFP subunit	*Desulfosporosinus* sp. BICA1-9	74%	391	WP_034140906
UF75_1958	KJR47680	506	RND-family efflux transporter protein, subunit AcrB	*Desulfosporosinus* sp. HMP52	91%	1033	WP_034600408
UF75_1959	WP_045574288	385	RND-family efflux transporter, MFP subunit	*Desulfosporosinus meridiei*	79%	388	WP_014902258

Table 2. *(Continued)*.

				Closest relative			
Gene ID	Accession no.	Size/aa	Predicted function	Organism	Identity	Size/aa	Accession no.
UF75_4355	WP_045576365	433	RND-family efflux transporter, MFP subunit	*Desulfosporosinus meridiei*	84%	431	WP_014904376
ABC-type zinc transporters							
UF75_0391	WP_045572900	264	Zinc ABC transporter, periplasmic-binding protein ZnuA	*Desulfosporosinus* sp. Tol-M	84%	306	WP_034616148
UF75_5078	WP_045576980	281	Zinc ABC transporter ZnuABC, permease component ZnuB	*Desulfosporosinus* sp. BICA1-9	95%	286	WP_034143107
UF75_5079	KJR44536	269	Zinc ABC transporter ZnuABC, ATP-binding protein ZnuC	*Desulfosporosinus* sp. BICA1-9	89%	246	WP_034140358
UF75_5080	WP_045576981	255	Zinc ABC transporter ZnuABC, periplasmic-binding protein ZnuA	*Desulfosporosinus* sp. BICA1-9	85%	311	WP_034143109
ZIP-family transporters							
UF75_1477	WP_045573871	246	Zinc transporter ZupT, ZIP family; divalent heavy-metal cations transporter	*Desulfosporosinus* sp. BICA1-9	89%	246	WP_034140358
UF75_3104	WP_045575306	247	Zinc transporter ZupT, ZIP family; divalent heavy-metal cations transporter	*Desulfosporosinus* sp. HMP52	91%	247	WP_034599480
CDF-family transporters							
UF75_1064	WP_045573500	332	Co/Zn/Cd cation transporter of the cation diffusion facilitator family transporters	*Desulfosporosinus* sp. BICA1-9	84%	332	WP_034146005
UF75_3098	WP_045575302	467	Co/Zn/Cd cation transporter of the cation diffusion facilitator family transporters	*Desulfosporosinus* sp. OT	78%	307	WP_009621334
Chromate transporters							
UF75_1302	WP_045573713	179	Chromate transporter ChrA	*Desulfosporosinus orientis*	80%	179	WP_014183400
UF75_1303	WP_045573714	175	Chromate transporter ChrA	*Desulfosporosinus* sp. HMP52	93%	175	WP_034598311
UF75_5439	KJR44178	256	Chromate transporter ChrA	*Desulfosporosinus* sp. BICA1-9	89%	419	WP_034144505
Arsenate resistance							
UF75_2367	WP_045574645	112	Arsenate reductase, ArsC family	*Desulfosporosinus* sp. BICA1-9	86%	112	WP_034140230
UF75_3204	WP_045575390	357	Arsenite efflux pump, membrane subunit ArsB	*Desulfosporosinus* sp. BICA1-9	97%	357	WP_034140747
UF75_3205	WP_045575391	108	DNA-binding transcriptional repressor ArsR	*Desulfosporosinus* sp. BICA1-9	92%	108	WP_034140748
UF75_3206	WP_045575392	578	Arsenite efflux pump, ATPase subunit ArsA	*Clostridium* sp. BNL1100	86%	580	WP_014314976

Table 2. *(Continued).*

Gene ID	Accession no.	Size/aa	Predicted function	Closest relative			
				Organism	Identity	Size/aa	Accession no.
UF75_3207	WP_045575393	128	Arsenical resistance operon trans-acting repressor ArsD	*Desulfitobacterium hafniense*	72%	129	WP_011461626
UF75_3208	WP_045575394	105	DNA-binding transcriptional repressor ArsR	*Desulfitobacterium dichloroeliminans*	76%	105	WP_015261303

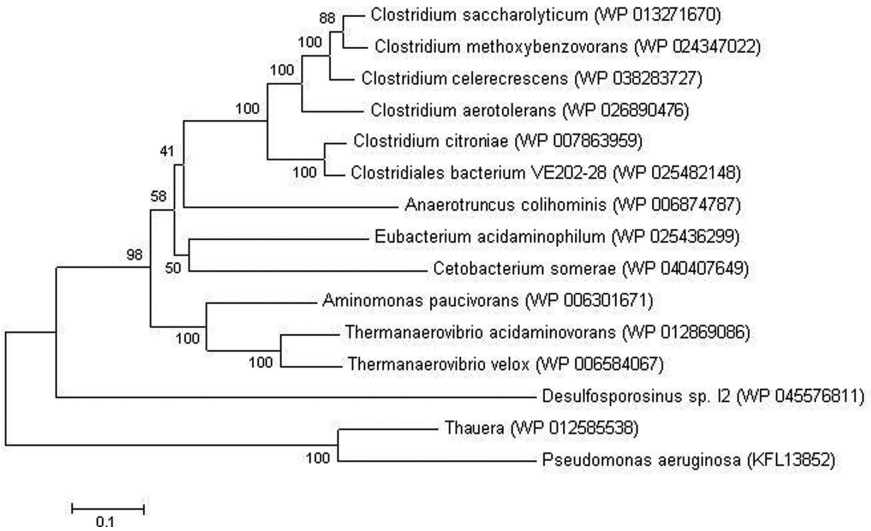

Figure 4. Phylogenetic tree showing the most closely related amino acid sequences to PPK 2 of *Desulfosporosinus* sp. I2. Numbers at branching points indicate bootstrap values determined from 1000 iterations.

transporting Zn^{2+}, Cd^{2+} and Pb^{2+} (UF75_0864, UF75_1937, UF75_3100, UF75_4472). It is noteworthy that other *Desulfosporosinus* sequenced genomes possess homologous metal transporters. No duplication or extended number of metal transporters were revealed in the I2 genome.

PolyP may play role in copper detoxification in strain I2. PolyP, the linear polymers of orthophosphate, have been associated with the capacity of microorganisms to tolerate various types of stresses and to chelate metals (Seufferheld, Alvarez and Farias 2008). The polyP association with vacuole-like bodies in strain I2 resembles bacterial acidocalcisomes, polyP storage organelles that were first described in eukaryotes but subsequently confirmed for various bacteria (Seufferheld *et al.* 2003). TEM micrographs of ultrathin sections of strain I2 showed that inclusions may be surrounded by a membrane. Although there were no vacuolar pyrophosphatase (H^+-V-PPase) homologs, a proton pump characteristic for both eukaryotic and bacterial acidocalcisomes was found in the genome. The key enzyme involved in bacterial polyP synthesis is polyphosphate kinase (PPK). The PPK-deficient mutants cannot tolerate acid stress (Kornberg, Rao and Ault-Riche 1999). Polyphosphate kinase 1 (PPK1) was not found in the I2 genome, although it contained a putative polyphosphate kinase 2 (PPK2) (UF75_4879). The latter protein had no homology in the available *Desulfosporosinus* genomes. Phylogenetic analysis shows that PPK2 from strain I2 was rather distant from all the known PPK2 and its closest relative with 30% similarity occurred in *Aminomonas paucivorans* from Synergistetes (Fig. 4).

PolyP can be associated with the cell wall. TEM micrographs of I2 showed that electron-dense fibrils may be associated with the cell wall. The genes for the proteins responsible for synthesis of gamma-poly-glutamate capsule were found in the genome. Although the UF75_0096 is annotated as D-Ala-D-Ala dipeptidase, it contains two domains. One of them is CapA, one of three membrane-associated enzymes in *Bacillus anthracis* that is required for synthesis of gamma-polyglutamic acid, a major component of the bacterial capsule. The second is D-alanyl-D-alanine dipeptidase domain.

The sophisticated cytoplasmic organization of strain I2 observed under TEM is in agreement with the occurrence in the genome actin-like proteins, Arp, that are considered as putative early PPKs (Whitehead *et al.* 2014), including MreB (UF75_4446), Mbl (UF75_2920) and ParM (UF75_0719). The proteins involved in microcompartments in the bacterial cell, including ethanolamine utilization protein (UF75_4231) also known as bacterial microcompartment domain repeat 2, were revealed in the genome.

Despite the relatively low tolerance to arsenic, strain I2 possesses the TRX-fold arsenate reductase ArsC that catalyzes the reduction of arsenate to arsenite (UF75_2367) and arsenite efflux pump, consisting of the catalytic ArsA subunit (UF75_3206) and the membrane subunit ArsB (UF75_3204). Nearly all sequenced *Desulfosporosinus* isolates have ArsC, but the entire efflux pump operon has been found only in strain I2 and *D. youngiae*.

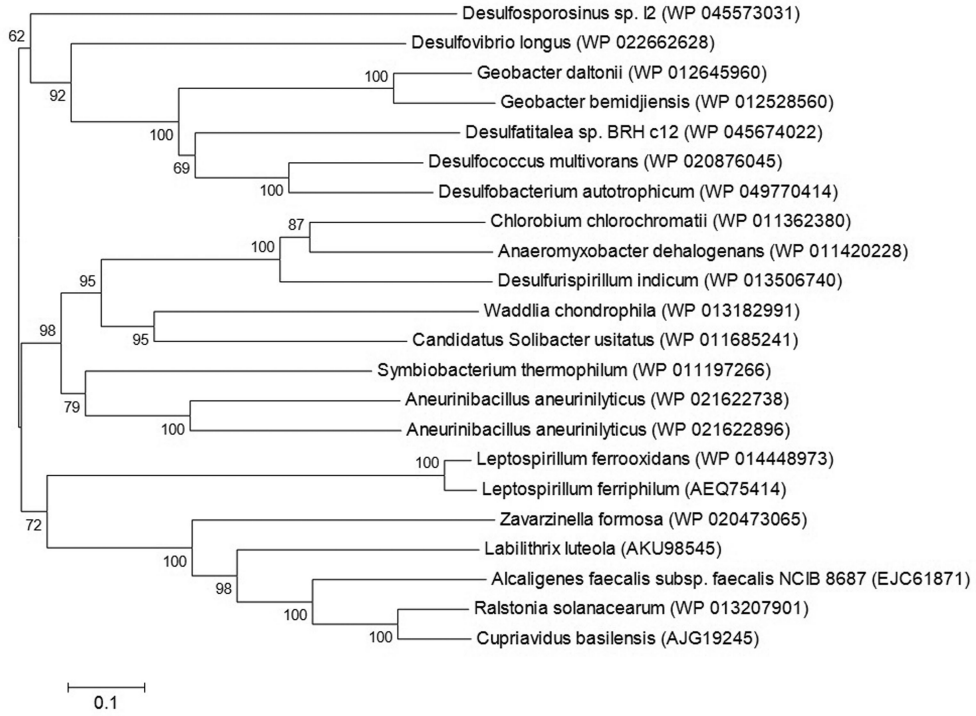

Figure 5. Phylogenetic tree showing the most closely related amino acid sequences to cbb3-type cytochrome *c* oxidase subunit I, which contains a heme-copper binuclear center and defines the membership in the superfamily. Numbers at branching points indicate bootstrap values determined from 1000 iterations.

Oxidative stress

In its natural environment, *Desulfosporosinus* sp. I2 may be frequently exposed to dissolved oxygen and thus should possess oxygen detoxification systems. We have identified superoxide dismutase (UF75_4309) and catalase (UF75_5085) genes in the I2 genome. These are typically found in aerobic bacteria, whereas anaerobes usually only employ superoxide reductase. The homologous catalase occurred in all six draft genomes of *Desulfosporosinus* species available in GenBank. In contrast, the superoxide dismutase homologs (UF75_4309) were found only in *D. meridei*, *D. youngiae* and two uncharacterized strains, *Desulfosporosinus* sp. BICA1-9 and *Desulfosporosinus* sp. HMP52. However, many Firmicutes possess the orthologous genes.

Terminal oxygen reductases in *Desulfosporosinus* sp. I2 are represented by a *cbb3*-type cytochrome *c* oxidase and a quinol oxidase *bd* complex. The first complex comprises subunits I (UF75_0563), II (UF75_0564) and III (UF75_0565). Subunit I contains multiple transmembrane helices. The other two subunits were predicted to carry N-terminal signal peptide, indicating its export from the cytoplasm and linking to the cell membrane. Interestingly, the *cbb3*-type cytochrome *c* oxidase does not occur in any other *Desulfosporosinus* except strain I2 and shares low similarity with its closest relatives in *Deltaproteobacteria* (Fig. 5). This cytochrome *c* oxidase belongs to the heme-copper transmembrane protein complexes. The *cbb3* is believed to be a modern enzyme that has evolved independently to perform a specialized function in microaerobic energy metabolism. The discovery, a copper-containing protein in *Desulfosporosinus* spp., which until recently has been considered to be strict anaerobes, is noteworthy. The recent comparative genomic studies suggest that the use of copper by prokaryotes is strongly linked to the use of oxygen (Ridge, Zhang and Gladyshev 2008; Karnachuk *et al.* 2015a) and the evolution of copper-containing proteins followed the oxygenation of the Earth (Ochiai 1983; Saito, Sigman and Morel 2003).

The second complex, the cytochrome *bd*-type quinol oxidase, consists of two subunits (UF75_2664 and UF75_2665) also carrying transmembrane helices. The *cbb3*-type and *bd*-type oxidases differ in their affinity to oxygen (e.g. Ekici *et al.* 2012) and thus together could protect cells from oxidative stress in fluctuating environment. Moreover, both cytochrome oxidases could reduce oxygen with electrons from the quinone pool and thus they may allow respiration of *Desulfosporosinus* sp. I2 under microaerophilic conditions. Our preliminary experiments showed that strain I2 did not grow under microaerobic conditions, when cells were cultivated in 12 ml stoppered vials containing liquid medium and 6 ml ambient air in the headspace. Further experiments are underway to examine the growth of the strain I2 in Hungate tubes with constant sparging of 0.02% oxygen and N_2 (Bukthyarova and Brasseur, unpublished data).

Low pH tolerance

Several mechanisms that allow microorganisms to withstand high extracellular proton concentrations have been reported (Baker-Austin and Dopson 2007). Interestingly, one of the most important systems participating in the generation of an internal positive membrane potential ($\Delta\psi$), the K^+-transporting Kdp ATPase, was not found in strain I2. Other three acidophilic sulfate-reducers, *D. acidiphilus*, *D. acididurans* and *Desulfosporosinus* sp. OT possess these genes. It is conceivable that the KdpABC proteins were lost for some reasons, because the regulation of the two-component histidine kinase KdpD (UF75_0351) occurred in I2 and was associated with two other K^+-transporting proteins, KtrB (UF75_0349) and TrkA (UF75_0348). Potassium-transport ATPases have been shown to be overrepresented in metagenomes from acidic environments (Jones *et al.* 2012). Additionally, the bac-

terium contained an acid resistance system exploiting proton-consuming decarboxylases, similar to those previously demonstrated in enterobacteria (Richard and Foster 2004; Fontenot *et al.* 2013), including arginine decarboxylase AdiA (UF75_RS17850) and lysine decarboxylase CadA (UF75_2412).

Carbon and nitrogen metabolism

Analysis of the genome *Desulfosporosinus* sp. I2 revealed genes encoding the complete Embden–Meyerhof pathway for glycolysis and gluconeogenesis: hexokinase (UF75_5178, UF75_0319), glucose-6-phosphate isomerase (UF75_5005), fructose 6-phosphate kinase (UF75_0114, UF75_3429, UF75_5006), fructose-1,6-bisphosphatase (UF75_2575), fructose bisphosphate aldolase (UF75_2577, UF75_3428), triose phosphate isomerase (UF75_3706), glyceraldehyde-3-phosphate dehydrogenase (UF75_3878, UF75_3437), phosphoenol pyruvate synthase (UF75_4789, UF75_1445, UF75_4126), 3-phosphoglycerate kinase (UF75_3436, UF75_3705), phosphoglycerate mutase (UF75_3707, UF75_3948), enolase (UF75_3708) and pyruvate kinase (UF75_3877). The inability of *Desulfosporosinus* sp. I2 to grow with glucose in sulfate medium suggests that the upper part of the Embden–Meyerhof pathway operates in the reverse direction of gluconeogenesis. The growth on glycerol is enabled by glycerol kinase (UF75_3704), the multisubunit glycerol-3-phosphate dehydrogenase (UF75_3701-3703) and downstream enzymes.

Complete oxidation of organic substrates could be enabled by the tricarboxylic acid (TCA) cycle, including citrate synthase (UF75_0595), aconitate hydratase (UF75_2731, UF75_3044), isocitrate dehydrogenase (UF75_3046, UF75_4848), 2-oxoglutarate oxidoreductase (UF75_0980- UF75_0983), succinyl CoA synthetase (UF75_1775, UF75_1773; UF75_2378, UF75_2379; UF75_2969, UF75_2970; UF75_3084, UF75_3085), succinate dehydrogenase (UF75_3086- UF75_3089; UF75_3017- UF75_3019), fumarate hydratase (UF75_4927-4928) and malate dehydrogenase (UF75_1777, UF75_3426).

Autotrophic CO_2 fixation could be performed through the Wood–Ljungdahl pathway (Ragsdale and Pierce 2008) including carbon monoxide dehydrogenase (UF75_0081, UF75_0341, UF75_1285, UF75_1521, UF75_1616), formate dehydrogenase (UF75_0475 (FdhD), UF75_4574 (FdhN), UF75_4575 (FdhI), UF75_4576 (FdhI)), formate-tetrahydrofolate ligase (UF75_1688), methylenetetrahydrofolate dehydrogenase (NADP+)/methenyltetrahydrofolate cyclohydrolase (UF75_0999), 5,10-methylenetetrahydrofolate reductase (UF75_1551, UF75_3484), 5-methyltetrahydrofolate:corrinoid iron–sulfur protein methyltransferase (UF75_1608), CODH/ACS (UF75_1609-UF75_1617) and acetate kinase (UF75_0903). However, growth of *Desulfosporosinus* sp. I2 with acetate and sulfate was not observed.

The genome of *Desulfosporosinus* sp. I2 contains all genes necessary for nitrogen fixation (Gussin, Ronson and Ausubel 1986). They are closely linked in the genome (UF75_0214-UF75_0223). To our knowledge, the capability to fix nitrogen has never been shown for *Desulfosporosinus,* although homologous genes occur in available *Desulfosporosinus* genomes. Nitrogen fixation was also revealed in the genome of a novel sulfate-reducing acidophilic Firmicute CEB3 (Petzsch *et al.* 2015a).

Respiratory electron transfer chains

All major components of an electron transfer chain able to generate transmembrane proton gradient are encoded in the *Desulfosporosinus* sp. I2 genome. The genome analysis revealed a putative membrane-bound complex similar to bacterial NADH:quinone oxidoreductase, respiratory complex I (Friedrich and Scheide 2000). There are two cluster of genes encoding NuoABCDHIJ subunits (UF_0875-UF_0869 and UF_4868-UF_4874), genes encoding NuoEFG (UF_1417-UF_1415), NuoKLM (UF75_5303-UF_5305) and NuoN (UF75_5036, UF75_5172). The succinate dehydrogenase complex is encoded by a three-gene operon and consists of an iron–sulfur subunit (UF_3017), a flavoprotein subunit (UF_3018) and a transmembrane cytochrome *b* subunit (UF_3019). The transmembrane ion gradient generated by electron transfer chains may be used for ATP synthesis by an F_0F_1-type ATPase, encoded by genes UF_2550-UF_2559.

Consistent with the ability of *Desulfospororsinus* sp. I2 to use sulfate for respiration, its genome contains the complete set of genes for dissimilatory sulfate reduction (Rabus, Hansen and Widdel 2007), including sulfate permease (UF75_2393, UF75_3177), sulfate adenylyltransferase (UF75_3182), Mn-dependent inorganic pyrophosphatase, two clusters of adenylsulfate reductase AprAB (UF75_0198/ UF75_0199 and UF75_3180/UF75_3181) and dissimilatory sulfite reductase (DsrA – UF75_3747, DsrB – UF75_3746, DsrC – UF75_3007). A two-gene operon encoding the subunits QmoA (UF75_3185) and QmoB (UF75_3184) of the adenylsulfate reductase-associated electron transfer complex QmoABC is located near the sulfate adenylyltransferase gene. However, the third gene, *qmoC* (encoding a quinone-interacting membrane-bound oxidoreductase), is absent, as also reported for the *qmo* operon in *Desulfotomaculum reducens* (Junier *et al.* 2010). Genes coding for sulfite reductase-associated electron transport proteins DsrMKJOP (DsrP – UF75_2291, UF75_3008, UF75_3985; DsrO – UF75_2292, UF75_3009, UF75_3175, UF75_ 3986; DsrJ – UF75_2279, UF75_3010; DsrK – UF75_3011, UF75_3750, UF75_0530; DsrM – UF75_3012, UF75_3751) are also present in the genome.

At least seven gene clusters coding for putative complex iron–sulfur molybdopterine (CISM) oxidoreductases of Psr/Psh family (reviewed by Rothery, Workun and Weiner 2008) are present in the genome. Such oxidoreductases usually comprise molybdopterin-binding catalytic subunit A, iron–sulfur electron transfer subunit B and the third subunit (C) linking this complex to the membrane and accepting the electrons from the quinone pool. The catalytic subunits (UF75_0346, UF75_0612, UF75_1326, UF75_2828, UF75_2884, UF75_3215, UF75_4739) are similar to the respective components of nitrate, thiosulfate, tetrathionate, sulfur, dimethyl sulfoxide and polysulfide reductases. Presumably, in *Desulfosporosinus* sp. I2 the CISM oxidoreductases can reduce some of these and/or other yet unknown electron acceptor(s), suggesting respiratory versatility of this bacterium.

In addition, the genome of *Desulfosporosinus* sp. I2 encodes NrfAH-type nitrite reductase, comprising electron transfer subunit NrfH (UF75_0062) and a catalytic subunit NrfA (UF75_0063). Both subunits are *c*-type cytochromes with four and five heme-binding motifs, respectively. However, the growth experiments showed that *Desulfosporosinus* sp. I2 did not grow with nitrite as an electron acceptor.

Hydrogenase and formate dehydrogenase genes

Five hydrogenases of the [NiFe]-family and two [FeFe]-family enzyme are present in the *Desulfosporosinus* sp. I2 genome along with two formate dehydrogenases. Although the ability of this strain to grow autotrophically on hydrogen and sulfate was not investigated, growth on formate and sulfate was observed.

Two [FeFe]-hydrogenases are encoded by gene clusters UF_1944-UF_1946 and UF_3768-UF_3770. The catalytic subunits UF_1944/UF_3770 contain the H-cluster domain (Vignais and Billoud 2007), and an additional N-terminal domain, which accommodates 2Fe–2S clusters. Two additional subunits, UF_1945/UF_3769 and UF_1946/UF_3768, are similar to the NuoF and NuoE subunits of NADH:quinone oxidoreductase, respectively. Their presence suggests that hydrogen reduction could be coupled to the oxidation of NAD(P)H. Another locus, UF_0436-UF_0439, contains similar NuoF and NuoE-like subunits associated with gene UF_0439 that encodes the catalytic alpha subunit of formate dehydrogenase. All these proteins lack N-terminal signal peptides or transmembrane domains, indicating their cytoplasmic localization. Subunit composition of the [FeFe]-hydrogenases of *Desulfosporosinus* sp. I2 is similar to that of the bifurcating hydrogenase from *Thermotoga maritima,* which simultaneously oxidizes NADH and ferredoxin to produce H_2 (Schut and Adams 2009). Similar bifurcating [FeFe]-hydrogenases and formate dehydrogenases have been identified in different sulfate-reducing Firmicutes, including *Desulfotomaculum kuznetsovii* and *Pelotomaculum thermopropionicum* (Müller *et al.* 2010; Visser *et al.* 2013). Such hydrogenases and formate dehydrogenases may link the oxidation of reduced ferredoxin and the unfavorable oxidation of NADH to produce hydrogen or formate.

Three group 1 [NiFe] uptake hydrogenases, each comprising small (UF_0627, UF_1035, UF_1897), large (UF_0628, UF_1034, UF_1896) and cytochrome *b* subunits (UF_0629, UF_1033, UF_1895), are probably linked to the cell membrane and oriented extracellularly, as evidenced by the presence of twin-arginine translocation motifs in the small subunits and multiple transmembrane helices in the cytochrome *b* subunits. These enzymes can oxidize H_2 and donate the electrons to the quinone pool. They can link the oxidation of H_2 to cytoplasmic sulfate reduction, with conservation of the energy in the form of a transmembrane proton gradient. A similar function is performed by the membrane-associated formate dehydrogenase, encoded by genes UF_4571, UF_4573 and UF_4575 (subunits alpha, beta and gamma, respectively). The enzyme catalyzes the oxidation of formate to carbon dioxide with the concomitant release of two electrons and two protons. The oxidation can be linked to sulfate respiration.

In addition, two group 4 [NiFe] hydrogenases are encoded (UF_0692-0697 and UF_0698-0703). These membrane-linked, six-subunit enzymes can dispose of the excess reducing equivalents generated by the anaerobic oxidation of organic compounds such as formate, and couple H_2 evolution and energy conservation by the generation of a transmembrane proton gradient (Vignais and Billoud 2007). The high number of hydrogenases and formate dehydrogenases in the genome of *Desulfosporosinus* sp. I2 indicates potentially high metabolic flexibility of this organism. This is important for changing growth strategies for example from sulfate respiration to syntrophic growth, although the latter mode has not been tested.

Motility and chemotaxis

Consistent with the observed motility of *Desulfosporosinus* sp. I2 cells, the genome contains a set of genes required for chemotaxis and flagellation. Flagellar motility is particularly important for *Desulfosporosinus* sp. I2, because it allows the cells to move towards favorable locations in terms of oxygen gradient in its natural environment. Most of the flagellar motility proteins are encoded by a single *fla* cluster (UF75_1808-1851). The flagellar motor rotation proteins are encoded by genes UF75_4497 (MotA) and UF75_4498 (MotB). At least 15 chemoreceptor proteins containing the transmembrane helices are encoded in the *Desulfosporosinus* sp. I2 genome. Other components of chemotaxis machinery in the genome are the signal transduction histidine protein kinase CheA (UF75_1838), its positive regulator CheW (UF75_1837, UF75_3836), response regulator methylesterase CheB (UF75_1836), CheY-P-specific phosphatase CheC (UF75_1814), chemoreceptor glutamine deamidase CheD (UF75_1813), chemotaxis protein methyltransferase CheR (UF75_0358, UF75_4501) and CheY signal receivers (UF75_1008, UF75_1824). Five copies of chemotaxis response regulators comprising a CheY-like receiver domain and a DNA-binding domain were identified (UF75_3169, UF75_3370, UF75_4113, UF75_4268, UF75_4968).

DISCUSSION

Cryptic sulfate reduction may occur in the oxidized mine wastes

The acidic pH and the high sulfate and metal concentrations of the pooled leachate, together with abundant yellow and red precipitates on rocks, and the dominance of secondary Fe(III)-hydroxysulfate minerals in the sediment, are clearly indicative of extensive sulfide oxidation in the tailings samples Xa201 and Xa202. Additionally, XRD-analysis showed very little indication of primary sulfide minerals in the sediment samples, but clearly demonstrated the presence of secondary minerals such as jarosite. These observations suggest that oxidation had resulted in the complete oxidation of primary sulfides in the upper layer of the tailings site. A positive redox potential was measured not only at the surface layer but also in the sediment interior at the depth of 3–4 cm.

The sulfate reduction rate in the oxidized Xa201 and Xa202 sediments was about the same order of magnitude as measured previously in the mining-impacted oxidized environments in Norilsk (Karnachuk *et al.* 2005). This rate may appear modest, but given the high sulfate concentrations in the oxic tailings, the absolute quantities of sulfate reduced under the oxic conditions and the accompanying precipitation of metals can reach substantial levels. Authigenic secondary sulfide minerals, recovered as a chromium-reducible sulfur fraction from the mine-impacted sediments in Norilsk, were enriched in ^{32}S compared to the primary sulfide $\delta^{34}S$ values, which testified to their biological origin (Karnachuk *et al.* 2005). At the same time, sulfides formed by SRB under oxidized conditions can undergo a relatively fast oxidation and thus cryptic sulfate reduction may occur in the upper layers of sulfide tailings.

Several previous studies have demonstrated the presence of SRB in the oxidized zone of sulfide tailings. Bruneel *et al.* (2005) discovered that the most abundant clone sequences retrieved from oxidized As-rich tailings in Cornoules (France) belonged to the class *Deltaproteobacteria*, which harbors many diverse SRB. In another study, a substantial number of clones related to the genera *Desulfobacterium* and *Desulfomonile* were retrieved from the fully oxygenated water of seepage from a tailings dam at the same mining site (Bruneel *et al.* 2006). Furthermore, culturable SRB have been regularly retrieved from the oxidized zones of various types of sulfide tailings (Fortin, Davis and Beveridge 1996, Fortin, Goulet and Roy 2000; Fortin *et al.* 2000; Diaby *et al.* 2007).

Desulfosporosinus spp. are important players in the sulfate reduction in acidic mine wastes

Our previous research of sulfate reduction at the Berikul site showed that *Desulfosporosinus* was the only phylotype with the known capability to reduce sulfate in the oxidized mine waste materials (Karnachuk *et al.* 2009). That is why the isolation procedure in this study targeted the spore-forming bacteria. Glycerol was used as a substrate for isolation because of the previous reports of possible toxicity of lactic acid and other organic acids under low pH conditions (Alazard *et al.* 2010; Meier, Piva and Fortin 2012; Sánchez-Andrea *et al.* 2014). Subsequently, it was discovered that strain I2 could grow with lactic acid as an electron donor. Lactic acid was used for isolation of another acidophilic *Desulfosporosinus* sp. BG from mine tailings in Transbaikal area (Karnachuk *et al.* 2015b). There are many reports of *Desulfosporosinus* detection in the biotopes associated with acidic mine environments (Nevin, Finneran and Lovley 2003; Petrie *et al.* 2003; Suzuki *et al.* 2003; Kimura, Hallberg and Johnson 2006; Rowe *et al.* 2007; Cardenas *et al.* 2008; Jin *et al.* 2008; Madden *et al.* 2009; Senko *et al.* 2009). Many of these reports rely on cultivation rather than on the use of molecular methods. Küsel *et al.* (2001) isolated *Desulfosporosinus* sp. Lau III from the acidic sediment of a lake impacted by strip coal mining. Labrentz and Banfield (2004) described the occurrence of culturable *Desulfosporosinus* spp. in a sulfide-precipitating biofilm in the Piquette Zn–Pb mine. The absence of *Desulfosporosinus*-related sequences in the clone libraries led them to suggest that the bacteria were in the sporulating phase, which hampered DNA isolation. Some of the novel SRB Firmicutes sequences retrieved by Winch *et al.* (2009) via preceding enrichment phases were from acidic tailings. We have previously isolated a pure culture *Desulfosporosinus* sp. DB from the Berikul tailings (Karnachuk *et al.* 2009). These observations imply that *Desulfosporosinus* may represent an important player in the sulfate-reducing community in the acidic environments. It is conceivable that *Desulfosporosinus*-related organisms in the sulfide tailings represent a 'rare biosphere', a phenomenon described for marine ecosystems (Sogin *et al.* 2006), when a low-abundance but active component of the community is masked by dominant populations.

Genomic insight does not reveal additional metal transporters in metal-tolerant *Desulfosporosinus* sp. I2

Desulfosporosinus sp. I2 habitat contained high concentrations of arsenic and the major mechanisms to tolerate it were present in the genome. However, the strain could not grow in the presence of more than 0.2 mM (15 mg l^{-1}) As, which is a lower concentration than known for the truly resistant strains. It is possible that As is effectively precipitated in the form of sulfides by SRB. Two different arsenic sulfides, orpiment and realgar, were found in the sediment samples from the tailings. It is possible that they were secondary sulfides formed due to As precipitation.

Desulfosporosinus sp. I2 could tolerate high copper levels of up to 142 mM. These levels are much higher than those reported for many metal-tolerant strains. For example, the model metal-tolerant *Cupriavidus metallidurans* has been reported to grow in the range of 1.5–12.5 mM Cu (Chen *et al.* 2008). A copper-resistant *Acidithiobacillus ferrooxidans*, an iron-oxidizing acidophile, could be adapted to up to 800 mM $CuSO_4$ (Navarro *et al.* 2009; Orellana and Jerez 2011). The presence of additional metal transporters is suggested as a general mechanism to withstand high metal concentrations. The genomic islands that combined different metal transporters have been reported for *C. metallidurans* (van Houdt *et al.* 2009) and *A. ferrooxidans* (Navarro *et al.* 2009; Orellana and Jerez 2011). The genome sequence of strain I2 did not reveal additional metal transporters as compared to the other sequenced *Desulfosporosinus* isolates. However, the level of metal tolerance among the *Desulfosporosinus* strains varied drastically, and other mechanisms may also play role in their metal resistance. One possible mechanism involves the sequestration via polyP. The transcriptome analysis, which is under way in our group, will help tackle the mechanisms involved in metal tolerance.

SUPPLEMENTARY DATA

Supplementary data are available at FEMSEC online.

ACKNOWLEDGEMENTS

This work was performed using the scientific equipment of the Core Research Facility 'Bioengineering' (Research Center of Biotechnology, Russian Academy of Sciences). We thank Andrei Miller and Olga Ikkert for their help with TEM. We also thank the editor and two anonymous reviewers for their comments, which helped to improve the manuscript.

FUNDING

The work was supported by the Ministry of Education and Sciences of the Russian Federation (FCP Program, Contract No. 14.604.21.0108, Project no. RFMEFI60414X0108).

Conflict of Interest. None declared.

REFERENCES

Abicht HK, Mancini S, Karnachuk OV *et al.* Genome sequence of *Desulfosporosinus* sp. OT, an acidophilic sulfate reducing bacterium from copper mining waste in Norilsk, Northern Siberia. *J Bacteriol* 2011;**193**:6104–5.

Abu Laban N, Tan B, Dao A *et al.* Draft genome sequence of uncultivated *Desulfosporosinus* sp. strain Tol-M, obtained by stable Isotope probing using [$^{13}C_6$]toluene. *Genome Announc* 2015;**3**, DOI: 10.1128/genomeA.01422-14.

Alazard D, Joseph M, Battaglia-Brunet F *et al.* *Desulfosporosinus acidiphilus* sp. nov.: a moderately acidophilic sulfate-reducing bacterium isolated from acid mining drainage sediments. *Extremophiles* 2010;**14**:305–12.

Baker-Austin C, Dopson M. Life in acid: pH homeostasis in acidophiles. *Trends Microbiol* 2007;**15**:165–71.

Banks D, Parnachev VP, Frengstad BS *et al.* Hydrochemical data report: the sampling of selected locations in the Republic of Khakassia, Kuznetsk Alatau Oblast' and Kemerovo Oblast', Southern Siberia, Russian Federation. *Norg Geol Unders Rep* 2008;**13**:1–60.

Bortnikova SB, Smolyakov BS, Sidenko NV *et al.* Geochemical consequences of acid mine drainage into a natural reservoir: inorganic precipitation and effects on plankton activity. *J Geochem Explor* 2001;**74**:127–39.

Brettin T, Davis JJ, Disz T *et al.* RASTtk: A modular and extensible implementation of the RAST algorithm for building custom annotation pipelines and annotating batches of genomes. *Sci Rep* 2015, DOI:10.1038/srep08365.

Bruneel O, Duran R, Casiot C *et al*. Diversity of microorganisms in Fe-As-rich acid mine drainage waters of Carnoulès, France. *Appl Environ Microb* 2006;**72**:551–6.

Bruneel O, Koffi K, Casiot C *et al*. Microbial diversity in pyrite-rich tailings impoundment (Carnoules, France). *Geomicrobiol J* 2005;**22**:1–9.

Cardenas E, Wu WM, Leigh MB *et al*. Microbial communities in contaminated sediments after bioremediation to submicromolar levels. *Appl Environ Microb* 2008;**74**:3718–29.

Chen WM, Wu CH, James EK *et al*. Metal biosorption capability of *Cupriavidus taiwanensis* and its effects on heavy metal removal by nodulation *Mimosa pudica*. *J Hazard Mater* 2008;**151**:364–71.

Cypionka H. Oxygen respiration by Desulfovibrio species. *Annu Rev Microbiol* 2000;**54**:827–48.

Diaby N, Dold B, Pfeifer H-R *et al*. Microbial communities in a porphyry copper tailings impoundment and their impact on the geochemical dynamics of the mine waste. *Environ Microbiol* 2007;**9**:298–307.

Dopson M, Johnson DB. Biodiversity, metabolism and applications of acidophilic sulfur-metabolizing microorganisms. *Environ Microbiol* 2012;**14**:2620–31.

Ekici S, Pawlik G, Lohmeyer E *et al*. Biogenesis of *cbb*(*3*)-type cytochrome c oxidase in *Rhodobacter capsulatus*. *Biochim Biophys Acta* 2012;**1817**:898–910.

Fontenot EM, Ezelle KE, Gabreski LN *et al*. YfdW and YfdU are required for oxalate-induced acid tolerance in *Escherichia coli* K-12. *J Bacteriol* 2013;**195**:1446–55.

Fortin D, Davis B, Beveridge TJ. The role of *Thiobacillus* and sulfate-reducing bacteria in iron biocycling in oxic and acidic mine tailings. *FEMS Microbiol Ecol* 1996;**21**:11–24.

Fortin D, Goulet R, Roy M. Seasonal cycling of Fe and S in a constructed wetland: the role of sulphate reducing bacteria. *Geomicrobiol J* 2000;**17**:221–35.

Fortin D, Roy M, Rioux J-P *et al*. Occurrence of sulfate-reducing bacteria under a wide range of physico-chemical conditions in Au and Cu-Zn mine tailings. *FEMS Microbiol Ecol* 2000;**33**:197–208.

Friedrich T, Scheide D. The respiratory complex I of bacteria, archaea and eukarya and its module common with membrane-bound multisubunit hydrogenases. *FEBS Lett* 2000;**479**:1–5.

Gieré R, Sidenko NV, Lazareva EV. The role of secondary minerals in controlling the migration of arsenic and metals from high-sulfide wastes (Berikul gold mine, Siberia). *Appl Geochem* 2003;**18**:1347–59.

Gussin G, Ronson C, Ausubel F. Regulation of nitrogen fixation genes. *Annu Rev Genet* 1986;**20**:567–91.

Ikkert OP, Gerasimchuk AL, Bukhtiyarova PA *et al*. Characterization of precipitates formed by H_2S-producing, Cu-resistant Firmicute isolates of *Tissierella* from human gut and *Desulfosporosinus* from mine waste. *Anton Van Lee* 2013;**103**:1221–34.

Jin S, Fallgren PH, Morris JM *et al*. Biological source treatment of acid mine drainage using microbial and substrate amendments: microcosm studies. *Mine Water Environ* 2008;**27**:20–30.

Jones DS, Albrecht HL, Dawson KS *et al*. Community genomic analysis of an extremely acidophilic sulfur-oxidizing biofilm. *ISME J* 2012;**6**:158–70.

Junier P, Junier T, Podell S *et al*. The genome of the Gram-positive metal- and sulfate-reducing bacterium *Desulfotomaculum reducens* strain MI-1. *Environ Microbiol* 2010;**12**:2738–54.

Karnachuk OV, Gavrilov SN, Avakyan MR *et al*. Diversity of cuproproteins and copper homeostasis systems in *Melioribacter roseus*, a facultatively anaerobic thermophilic member of a new phylum *Ignavibacteriae*. *Mikrobiologiya* 2015a;**84**:165–74.

Karnachuk OV, Gerasimchuk AL, Stykon GA *et al*. Bacteria of the sulfur cycle in the sediments of gold mine tailings, Kuznetsk Basin, Russia. *Mikrobiologiya* 2009;**78**:483–91.

Karnachuk OV, Kurganskaya IA, Avakyan MR *et al*. An acidophilic *Desulfosporosinus* isolated from the oxidized mining wastes in the Transbaikal area. *Mikrobiologiya* 2015b;**84**:595–605.

Karnachuk OV, Mardanov AV, Avakyan MR *et al*. Draft genome sequence of the first acid-tolerant sulfate-reducing deltaproteobacterium *Desulfovibrio* sp. TomC having potential for minewater treatment. *FEMS Microbiol Lett* 2015c;**362**:1–3.

Karnachuk OV, Pimenov NV, Iusupov SK *et al*. Distribution, diversity, and activity of sulfate-reducing bacteria in the water column in Gek-Gel Lake, Azerbaijan. *Mikrobiologiya* 2006;**75**:101–9.

Karnachuk OV, Pimenov NV, Yusupov SK *et al*. Sulfate reduction potential in sediments in the Norilsk mining area, Northern Siberia. *Geomicrobiol J* 2005;**22**:11–25.

Karnachuk OV, Sasaki K, Gerasimchuk AL *et al*. Precipitation of Cu-sulfides by copper-tolerant *Desulfovibrio* isolates. *Geomicrobiol J* 2008;**25**:219–27.

Kimura S, Hallberg KB, Johnson DB. Sulfidogenesis in low pH (3.8-4.2) media by a mixed population of acidophilic bacteria. *Biodegradation* 2006;**17**:159–67.

Kornberg A, Rao NN, Ault-Riche D. Inorganic polyphosphate: a molecule of many functions. *Annu Rev Biochem* 1999;**68**:89–125.

Küsel K, Roth U, Trinkwalter T *et al*. Effect of pH on the anaerobic microbial cycling of sulfur in mining-ompacted freshwater lake sediments. *Environ Exp Bot* 2001;**46**:213–23.

Labrenz M, Banfield JF. Sulfate-reducing bacteria-dominated biofilms that precipitate ZnS in a subsurface circumneutral-pH mine drainage. *Microb Ecol* 2004;**47**:205–17.

Lagesen K, Hallin PF, Rødland E *et al*. RNAmmer: consistent and rapid annotation of ribosomal RNA genes. *Nucleic Acids Res* 2007;**35**:3100–8.

Lowe TM, Eddy SR. tRNAscan-SE: a program for improved detection of transfer RNA genes in genomic sequence. *Nucleic Acids Res* 1997;**25**:955–64.

Madden AS, Palumbo AV, Ravel B *et al*. Donor-dependent extent of uranium reduction for bioremediation of contaminated sediment microcosms. *J Environ Qual* 2009;**38**:53–60.

Mancini S, Abicht HK, Karnachuk OV *et al*. Genome sequence of *Desulfovibrio* sp. A2, a highly copper resistant, sulfate-reducing bacterium isolated from effluents of a zinc smelter at the Urals. *J Bacteriol* 2011;**193**:6793–4.

Meier J, Piva A, Fortin D. Enrichment of sulfate-reducing bacteria and resulting mineral formation in media mimicking pore water metal ion concentrations and pH conditions of acidic pit lakes. *FEMS Microbiol Ecol* 2012;**79**:69–84.

Mori K, Kim H, Kakegawa T *et al*. A novel lineage of sulfate-reducing microorganisms: *Thermodesulfobiaceae* fam. nov., *Thermodesulfobium narugense*, gen. nov., sp. nov., a new thermophilic isolate from a hot spring. *Extremophiles* 2003;**7**:283–90.

Müller N, Worm P, Schink B *et al*. Syntrophic butyrate and propionate oxidation processes: from genomes to reaction mechanisms. *Environ Microbiol Rep* 2010;**2**:489–99.

Ňancucheo I, Johnson DB. Removal of sulfate from extremely acidic mine waters using low pH sulfidogenic bioreactors. *Hydrometallurgy* 2014;**150**:222–6.

Navarro CA, Orellana LH, Mauriaca C *et al*. Transcriptional and functional studies of *Acidithiobacillus ferrooxidans* genes related to survival in the presence of copper. *Appl Environ Microb* 2009;**75**:6102–9.

Nevin KP, Finneran KT, Lovley DR. Microorganisms associated with uranium bioremediation in a high-salinity subsurface sediment. *Appl Environ Microb* 2003;**69**:3672–5.

Nies DH. Efflux-mediated heavy metal resistance in prokaryotes. *FEMS Microbiol Rev* 2003;**27**:313–39.

Ochiai E. Copper and the biological evolution. *Biosystems* 1983;**16**:81–6.

Orellana LH, Jerez CA. A genomic island provides *Acidithiobacillus ferrooxidans* ATCC 53993 additional copper resistance: a possible competitive advantage. *Appl Microbiol Biot* 2011;**92**:761–7.

Parks DH, Imelfort M, Skennerton CT *et al*. CheckM: assessing the quality of microbial genomes recovered from isolates, single cells, and metagenomes. *Genome Res* 2015;**25**:1043–55.

Pester M, Brambilla E, Alazard D *et al*. Complete genome sequences of *Desulfosporosinus orientis DSM765*^{T}, *Desulfosporosinus youngiae DSM17734*^{T}, *Desulfosporosinus meridiei DSM13257*^{T}, *and Desulfosporosinus acidiphilus DSM22704*^{T}. *J Bacteriol* 2012;**194**:6300–1.

Petrie L, North NN, Dollhopf SL *et al*. Enumeration and characterization of iron(III)-reducing microbial communities from acidic subsurface sediments contaminated with uranium(VI). *Appl Environ Microb* 2003;**69**:7467–79.

Petzsch P, Poehlein A, Johnson DB *et al*. Genome sequence of the acidophilic sulfate-reducing *Peptococcaceae* strain CEB3. *Genome Announc* 2015a, DOI: 10.1128/genomeA.00886-15.

Petzsch P, Poehlein A, Johnson DB *et al*. Genome sequence of the moderately acidophilic sulfate-reducing Firmicute *Desulfosporosinus acididurans* (strain M1T). *Genome Announc* 2015b, DOI: 10.1128/genomeA.00881-15.

Rabus R, Hansen T, Widdel F. Dissimilatory sulfate-and sulfur-reducing prokaryotes. In: Dworkin M (ed.). *The Prokaryotes*. New York: Springer, 2007, 659–768.

Ragsdale SW, Pierce E. Acetogenesis and the Wood-Ljungdahl pathway of CO_2 fixation. *Biochim Biophys Acta* 2008;**1784**:1873–98.

Ramel F, Brasseur G, Pieulle L *et al*. Growth of the obligate anaerobe *Desulfovibrio vulgaris* Hildenborough under continuous low oxygen concentration sparging: impact of the membrane-bound oxygen reductases. *PLoS One* 2015, DOI: 10.1371/journal.pone.0123455.

Richard H, Foster JW. *Escherichia coli* glutamate- and arginine-dependent acid resistance system increase internal pH and reverse transmembrane potential. *J Bacteriol* 2004;**186**:6032–41.

Ridge PG, Zhang Y, Gladyshev VN. Comparative genomic analyses of copper transporters and cuproproteomes reveal evolutionary dynamics of copper utilization and its link to oxygen. *PLoS One* 2008, DOI: 10.1371/journal.pone.0001378.

Rothery RA, Workun GJ, Weiner JH. The prokaryotic complex iron-sulfur molybdoenzyme family. *Biochim Biophys Acta* 2008;**1778**:1897–929.

Rowe OF, Sánchez-España J, Hallberg K *et al*. Microbial communities and geochemical dynamics in an extremely acidic, metal-rich stream at an abandoned sulfide mine (Huelva, Spain) underpinned by two functional primary production systems. *Environ Microbiol* 2007;**9**:1761–71.

Saito MA, Sigman DM, Morel FMM. The bioinorganic chemistry of the ancient ocean: the co-evolution of cyanobacterial metal requirements and biogeochemical cycles at the Archean/Proterozoic boundary? *Inorg Chim Acta* 2003;**356**:308–18.

Sánchez-Andrea I, Knittel K, Amann R *et al*. Quantification of Tinto River sediment microbial communities: importance of sulfate-reducing Bacteria and their role in attenuating acid mine drainage. *Appl Environ Microb* 2012;**78**:4638–45.

Sánchez-Andrea I, Sanz JL, Bijmans MFM *et al*. Sulfate reduction at low pH to remediate acid mine drainage. *J Hazard Mater* 2014;**269**:98–109.

Sánchez-Andrea I, Stams AJM, Hedrich S *et al*. *Desulfosporosinus acididurans* sp. nov.: an acidophilic sulfate-reducing bacterium isolated from acidic sediments. *Extremophiles* 2015;**19**:39–47.

Schut GJ, Adams MW. The iron-hydrogenase of *Thermotoga maritima* utilizes ferredoxin and NADH synergistically: a new perspective on anaerobic hydrogen production. *J Bacteriol* 2009;**191**:4451–57.

Senko JM, Zhang G, McDonough JT *et al*. Metal reduction at low pH by a *Desulfosporosinus* species: implications for the biological treatment of acidic mine drainage. *Geomicrobiol J* 2009;**26**:71–82.

Seufferheld MJ, Alvarez HM, Farias ME. Role of polyphosphates in microbial adaptation to extreme environments. *Appl Environ Microb* 2008;**74**:5867–74.

Seufferheld MJ, Vieira MC, Ruiz FA *et al*. Identification of organelles in bacteria similar to acidocalcisomes of unicellular eukaryotes. *J Biol Chem* 2003;**278**:29971–8.

Sidenko NV, Bortnikova SB, Lazareva EV *et al*. Geochemical and mineralogical zoning of high-sulfide mine waste at the Berikul mine site, Kemerovo region, Russia. *Can Mineral* 2005;**43**:1141–56.

Sogin ML, Morrison HG, Huber JA *et al*. Microbial diversity in the deep sea and the underexplored "rare biosphere". *P Natl Acad Sci USA* 2006;**103**:12115–20.

Suzuki Y, Kelly SD, Kemner KM *et al*. Microbial populations stimulated for hexavalent uranium reduction in uranium mine sediment. *Appl Environ Microb* 2003;**69**:1337–46.

van Houdt R, Monchy S, Leys N *et al*. New mobile genetic elements in *Cupriavidus metallidurans* CH34, their possible roles and occurrence in other bacteria. *Anton Van Lee* 2009;**96**:205–26.

Vignais PM, Billoud B. Occurrence, classification, and biological function of hydrogenases: an overview. *Chem Rev* 2007;**107**:4206–72.

Visser M, Worm1 M, Muyzer G *et al*. Genome analysis of *Desulfotomaculum kuznetsovii* strain 17T reveals a physiological similarity with *Pelotomaculum thermopropionicum* strain SI^T. *Stand Genom Sci* 2013;**8**:69–87.

Whitehead MP, Eagles L, Hooley P *et al*. Most bacteria synthesize polyphosphate by unknown mechanisms. *Microbiology* 2014;**160**:829–31.

Widdel FF, Bak R. Gram-negative mesophilic sulfate-reducing bacteria. In: Balows A (ed.). *The Prokaryotes*. Berlin: Springer, 1992, 3352–78.

Winch S, Mills HJ, Kostka JE *et al*. Identification of sulfate-reducing bacteria in methylmercury-contaminated mine tailings by analysis of SSU rRNA genes. *FEMS Microbiol Ecol* 2009;**68**:94–107.